Eur Biophys J (2002) 31: 417–427
DOI 10.1007/s00249-002-0230-6

ARTICLE

**Ida C. Bonini · Silvia S. Antollini**
**Carlos Gutiérrez-Merino · Francisco J. Barrantes**

# Sphingomyelin composition and physical asymmetries in native acetylcholine receptor-rich membranes

Received: 8 January 2002 / Revised: 4 April 2002 / Accepted: 8 April 2002 / Published online: 14 June 2002


**Abstract** Selective enzymatic hydrolysis, lipid compositional analyses, and fluorescence studies have been carried out on acetylcholine receptor (AChR)-rich membranes from Torpedinidae to investigate the topology of sphingomyelin (SM) in the native membrane and its relationship with the AChR protein. Controlled sphingomyelinase hydrolysis of native membranes showed that SM is predominantly (~60%) localized in the outer half of the lipid bilayer. Differences were also observed in the distribution of SM fatty acid molecular species in the two bilayer leaflets. A fluorescent SM derivative {*N*-[10-(1-pyrenyl)decanoyl]sphingomyelin; Py-SM} was used to study protein-lipid interactions in the AChR-rich membrane and in affinity-purified *Torpedo* AChR reconstituted in liposomes made from *Torpedo* electrocyte lipid extracts. The efficiency of Förster resonance energy transfer (FRET) from the protein to the pyrenyl-labeled lipid as a function of acceptor surface density was used to estimate distances and topography of the SM derivative relative to the protein. The dynamics of the lipid acyl chains were explored by measuring the thermal dependence of Py-SM excimer formation, sensitive to the fluidity of the membrane. Differences were observed in the concentration dependence of excimer/monomer pyrenyl fluorescence when measured by direct excitation of the probe as against under FRET conditions, indicating differences in the intermolecular collisional frequency of the fluorophores between bulk and protein-vicinal lipid environments, respectively. Py-SM exhibited a moderate selectivity for the protein-vicinal lipid domain, with a calculated relative affinity $K_r \approx 0.55$. Upon sphingomyelinase digestion of the membrane, FRET efficiency increased by about 50%, indicating that the resulting pyrenylceramide species have higher affinity for the protein than the parental SM derivative.

**Keywords** Sphingolipids · Membrane lipids · Fluorescence · Energy transfer

I.C. Bonini · S.S. Antollini · F.J. Barrantes (✉)
UNESCO Chair of Biophysics
and Molecular Neurobiology/Instituto de Investigaciones
Bioquímicas de Bahía Blanca, 8000 Bahía Blanca, Argentina
E-mail: rtfjb1@criba.edu.ar
Tel.: +54-291-4861201
Fax: +54-291-4861200

C. Gutiérrez-Merino
Departamento de Bioquímica y Biología Molecular,
Universidad de Extremadura, Spain

## Introduction

The major lipid components of biological membranes are phosphoglycerides, cholesterol, and sphingolipids. Sphingomyelins (*N*-acylsphingosine-1-phosphorylcholine or ceramide-1-phosphorylcholine) (SMs), the simplest class of the sphingolipids, amount to about 10% of phospholipids of mammalian cell membranes. As with phosphatidylcholine (PC), the other choline-containing phospholipid, SMs occur mostly in the plasma membrane of the outer, exoplasmic leaflet of the bilayer (Barenholz and Thompson 1980; Koval and Pagano 1991). Aminophospholipids such as phosphatidylserine (PS) and phosphatidylethanolamine (PE), on the other hand, predominate in the inner, cytoplasmic leaflet of the membrane (Devaux 1992). SM is also purported to play a key role in the so-called "SM cycle" (Hannun and Obeid 1995), in which SM-derived ceramide acts as a second messenger lipid in apoptosis.

Another rapidly developing area in which the participation of SM appears to play a crucial role is that of cholesterol-SM microdomains or "rafts". These special lipid domains are postulated to result from the strong and preferential interactions between the two lipid species, resulting in lateral segregation in the plane of the membrane (Brown 1998; Jacobson and Dietrich 1999). Lipid rafts have been implicated to participate in processes such as cell signaling, and sorting and trafficking of some membrane proteins to the cell surface.

In the case of the nicotinic acetylcholine receptor (AChR)-rich membranes obtained from the electric

organ of Torpedinidae species, the major phospholipid constituents are PC (40%), PE (35%), and PS (13%), whereas SM accounts for about 5% of total phospholipid content (González-Ros et al. 1982; Bonini de Romanelli et al. 1987; Rotstein et al. 1987). Its location on the cell surface membrane is not known, nor has it been determined whether its presence has any structural and/or functional significance with respect to the major functional entity in this membrane, i.e. the AChR. The occurrence of protein-associated or "annular" lipids, relatively immobile with respect to the rest of the lipids in the native membrane environment (Marsh and Barrantes 1978; Marsh et al. 1981) on the one hand, and the high cholesterol content of the native AChR membrane on the other (González-Ros et al. 1982; Rotstein et al. 1987), raises the possibility that the membrane regions where receptor clusters occur, and where lipid composition is apparently different (Scher and Bloch 1993), could also be enriched in SM.

Pyrene derivatives have been extensively used to probe protein structure and dynamics, and in a few cases pyrenyl fluorescent probes have been especially designed for study of the cholinergic system (Barrantes et al. 1975). Pyrene azide has been used to label the AChR in its native membrane environment (Marquez et al. 1989) and purified *Torpedo* AChR labeled in γCys451 with *N*-(1-pyrenyl)maleimide has helped to establish an average distance of about 18 Å between donor Trp residue(s) in the AChR and the covalently bound pyrene ring (Narayanaswami et al. 1993). Interestingly, γTrp453, also located in the M4 transmembrane region and certainly very close to γCys451, is the only Trp residue present in the whole AChR membrane-spanning domain out of a total of 51 *Torpedo* AChR tryptophan residues, and is considered to be the major tryptophanyl energy transfer donor to membrane-embedded probes owing to its close vicinity. More recently, Barrantes et al. (2000) have labeled intact *T. californica* AChR protein and transmembrane peptides αM1, αM4, γM1, and γM4 with *N*-(1-pyrenyl)maleimide, to study the topography of the pyrene-labeled Cys residues with respect to the membrane and the apparent affinity for representative lipids. Differential fluorescence quenching with spin-labeled lipids was used to determine the shallow location of the Cys residues (Barrantes et al. 2000). *Discopyge tschudii*, a related Torpedinidae found in the South Atlantic, exhibits a very similar primary structure (Lacorazza et al. 1996) and is likely to display analogous topology.

Here we have investigated the distribution of SM and its fatty acid constituents in the intact AChR-rich membrane, and the topographical relationship between this choline-containing sphingolipid and the AChR by a combination of biochemical and fluorescence spectroscopy techniques. The former provides evidence of an asymmetry of SM and its fatty acyl chains between the exofacial and cytoplasmic leaflets of the membrane. In the fluorescence studies, we used *N*-[10-(1-pyrenyl)decanoyl]sphingomyelin (Py-SM) as a reporter group of the lipid physical state. The presence of the AChR protein is shown to hinder excimer formation of the pyrenyl lipid, since the protein-adjacent, "annular" lipid exhibited restricted Py-SM mobility relative to that of the bulk bilayer lipid, as measured by Förster resonance energy transfer (FRET), the nonradiative process by which energy is transferred from an emitting fluorophore (the donor) to a suitable acceptor by long-range dipole-dipole coupling. Furthermore, FRET is also exploited to measure the topographical relationship between the protein and the protein-adjacent fluorescent lipid analog and their relative affinity. Py-SM is shown to have a moderate selectivity for the AChR-associated lipid domain. The combined data provide evidence of the asymmetry of SM between exofacial and cytoplasmic membrane leaflets as well as lateral structural and dynamic segregation between protein-associated and bulk lipid regions, respectively.

## Materials and methods

### Materials

*D. tschudii* electric fish (Torpedinidae belonging to the superfamily Narcinoidae) were captured near the South Atlantic coast at Necochea, Argentina, and transported by ground in sealed plastic bags containing seawater and oxygen. *T. marmorata* specimens were obtained either from the Roscoff marine station in France, or from the Mediterranean coast off Alicante, Spain. The latter were kindly provided by Dr. J.M. González-Ros. On arrival the fish were killed by pithing and the electric organs dissected and stored at –70 °C until further use. SM from bovine brain, SMase (sphingomyelin phosphodiesterase, EC 3.1.4.12) from *Bacillus cereus*, *N*-[10-(1-pyrenyl)decanoyl]sphingomyelin, HEPES, and EDTA were obtained from Sigma (St. Louis, Mo., USA).

### Preparation of AChR-rich membranes

Membrane fragments rich in AChR were prepared as previously described (Barrantes 1982). Typically, *T. marmorata* and *D. tschudii* AChR-rich membrane fragments had specific activities in the order of 3.040 and 1.500 pmol α-bungarotoxin sites/mg protein, respectively.

### Integrity and sidedness of AChR vesicles

More than 80% of native AChR-rich membranes form closed vesicles (Bonini de Romanelli et al. 1990; Gutiérrez-Merino et al. 1995). The orientation of AChR in these vesicles was measured as described by Hartig and Raftery (1979) by determining the total toxin binding sites in the presence of Triton X-100 and the right-side-out toxin binding sites in the absence of detergent, as in previous work from our laboratory (Bonini de Romanelli et al. 1990; Gutiérrez-Merino et al. 1995).

### Purification and reconstitution of the AChR

AChR was affinity purified from frozen electric tissue from *T. marmorata* on an immobilized-bromoacetylcholine Affi-Gel 10 column (Venera et al. 1997). The receptor was stored at –70 °C in 10 mM phosphate buffer containing 100 mM NaCl, 0.1 mM EDTA, 0.02% $NaN_3$ (pH 7.4). For reconstitution, *Torpedo* lipid extracts and different amounts of Py-SM dissolved in buffer A (20 mM HEPES, pH 7.4, containing 150 mM NaCl and 0.25 mM $MgCl_2$) containing 1% cholate were mixed with the purified

receptor in a lipid to protein molar ratio of about 250:1. The mixtures were dialyzed at 4 °C for 48 h against four changes of buffer A. Samples with and without Py-SM were used immediately after dialysis in fluorescence measurements.

### Preparation of liposomes

Liposomes were prepared from endogenous lipids extracted from AChR-rich membranes. They were obtained by resuspending the mixed dried lipid in buffer A to give a final concentration of 1 mg $mL^{-1}$. The lipid dispersion was sonicated to clarity with a Branson ultrasonic sonifier.

### Phospholipase treatment

SMase treatment was carried out essentially as described in Vénien and Le Grimellec (1988), with a few modifications. Membrane fragments rich in AChR (final concentration 1.25 mg protein $mL^{-1}$) were dispersed in buffer A. The reaction was started by adding 0.5 U SMase/mg protein to the vesicle suspension. Incubation was carried out at 37 °C with gentle shaking. Aliquots were taken at increasing intervals and the reaction was stopped by addition of EDTA (Boegheim et al. 1983). In another series of experiments, native AChR-rich membrane fragments were dispersed and incubated with the enzyme as described above after 30 min of treatment with 0.06% saponin at 22 °C (Gutiérrez-Merino et al. 1995). For each experimental design, control samples were treated identically except that SMase was omitted from the incubation mixture. SMs were separated by two-dimensional thin-layer chromatography on silica gel H with the solvent system described by Rouser et al. (1970) and located by exposure to iodine vapor. The spots were scraped off and transferred to tubes for determination of lipid phosphorus (Rouser et al. 1970).

### Analysis of fatty acids in SMs and ceramides of AChR membrane

AChR membranes were treated with SMase, and SMs were separated as described above. Ceramides were isolated with monodimensional thin-layer chromatography using silica gel G plates and chloroform/methanol/acetic acid (20:1:0.15, by vol) as developing system (Roelofsen 1982). Both lipids were identified with 2′,7′-dichlorofluorescein and the spots were located under ultraviolet light and eluted by the method of Arvidson (1968). Methyl esters were prepared according to Morrison and Smith (1964) and purified by monodimensional chromatography on silica gel G plates previously washed with a mixture of chloroform/methanol/acetone (1:1:1, by vol) containing 1% water. The developing solvents were hexane/ether (9:1, v/v). Spots were located and eluted as described above and the resulting samples analyzed by gas-liquid chromatography. Two glass columns (2 m×2 mm i.d.) packed with 15% OV-275 on 80–120 Chromosorb WAW (Varian, Sunnyvale, Calif., USA) were connected to two flame ionization detectors operated in the dual-differential mode. A linear (5 °C $min^{-1}$) temperature program, starting at 160 °C and ending at 220 °C, was used.

### Other biochemical procedures

Protein content was determined by the method of Lowry et al. (1951). Total lipids were extracted by the method of Folch et al. (1957) or Bligh and Dyer (1959).

### Fluorescence spectroscopy

Fluorescence spectra were recorded with an SLM Aminco 4800 spectrofluorimeter using 10×10 mm quartz cuvettes. The AChR-rich membrane samples in buffer A (50 μg protein $mL^{-1}$), having an OD < 0.1, were labeled with Py-SM in ethanol and incubated for 40–60 min at room temperature in the dark. The amount of organic solvent added was kept in all cases below 0.5%. After incubation, the samples were centrifuged at 45,000 rpm at 4 °C for 1 h in order to eliminate excess probe. The resulting pellet was resuspended in buffer A by forcing the suspension through the needle of a small syringe. In order to calculate the exact amount of Py-SM in the membrane, the following experiment was carried out: after centrifugation, lipids were extracted as given above from the pellet and supernatant, respectively. The extracted lipids were resuspended in ethanol, their absorbance measured at 342 nm, and compared with a standard curve of Py-SM in ethanol. Nearly 35% of the added Py-SM was effectively incorporated in the membrane. The excitation wavelength was set at 290 or 346 nm with a slit width of 5 nm for fluorescence resonance energy transfer (FRET) conditions and direct excitation of the pyrenyl derivative, respectively. Emission spectra were corrected for wavelength-dependent distortions and dilution effects. Inner filter effects were small, and were corrected as described by Lakowicz (1999) and Homan and Eisenberg (1985). Correction of the inner filter effect also implicitly takes into account the turbidity of AChR membranes (OD < 0.1). All experiments were carried out at 20 °C except for those in which the temperature dependence of the fluorescence emission was being studied, in which case this parameter was kept within 0.2 °C in the range 5–45 °C with a circulating thermostatted water bath (Haake, Darmstadt, Germany). Experiments in which the effect of SMase was tested were conducted at 37 °C.

### Energy transfer experiments

The samples were excited at 290 nm and emission spectra recorded in the 300–600 nm range. Protein, pyrene monomer, and excimer emission maxima at about 330, 374, and 472 nm, respectively, were used in the calculations. When the excimer/monomer ($F_E/F_M$) ratio was measured under FRET conditions, the contribution of the protein emission at 374 nm, overlapping with the pyrene monomer emission, was corrected by subtracting the normalized spectrum of AChR-rich membrane at 330 nm in the absence of Py-SM (see e.g. Fig. 2). Another series of control $F_E/F_M$ measurements was carried out using Py-SM in liposomes prepared from endogenous AChR-rich membranes.

### Energy transfer efficiency

The efficiency of the resonance energy transfer ($E$) in relation to all other deactivation processes of the excited donor was calculated by assessing the degree of donor (intrinsic fluorescence) quenching as:

$$E = 1 - (\phi/\phi_D) = 1 - (I/I_D) \quad (1)$$

where $\phi$ and $\phi_D$ are the fluorescence quantum yields of donor in the presence and absence of the acceptor, respectively, and $I$ and $I_D$ are the corresponding emission intensities in any given measurement. Here $I$ and $I_D$ correspond to the maximal intrinsic protein emission intensity, 330 nm, in the presence and absence of acceptor, respectively. Ethanol was found to produce quenching of the fluorescence. Control experiments were thus performed in all cases with addition of ethanol only, in the absence of the fluorescence probe, and $E$ corrected for ethanol quenching.

The analysis of the $E$ was carried out as indicated in Gutiérrez-Merino et al. (1987, 1989). Briefly, the overall energy transfer of the ensemble can be computed as the sum of the energy transfer occurring between individual donor-acceptor pairs in the two-dimensional membrane system (the lipid bilayer), i.e. $< K > = \Sigma k_i$, where the rate of transfer for pair $i$ separated by a distance $r_i$ is $k_i$. This expression has been used to measure relative positions of protein and lipid in a mixture (Gutiérrez-Merino et al. 1987, 1989), and is based on a model of the distribution of both donor and acceptor molecules as a continuum of discs of different sizes. Random and non-random distribution (i.e. preferential binding) of Py-SM in the AChR annular lipid was introduced into the calculation.

Experimentally, measurements of the extent of quenching of donor fluorescence by Förster energy transfer were carried out in

the absence and presence of increasing concentrations of Py-SM. The values of the energy transfer efficiency for different acceptor surface densities were calculated by parametric fitting of theoretical predictions of FRET to the experimental data as a function of $r$, $H$, and $K_r$, with an $R_0$ value of $21 \pm 2$ Å (see Results), weighting the probability of occurrence of donor/acceptor pairs at the lipid belt region relative to that of a random distribution (Gutiérrez-Merino et al. 1987; Antollini et al. 1996). The distance of closest approach ($d$) between donor (ensemble of donor Trp residues in the AChR molecule)-acceptor (Py-SM molecules) pairs is given in terms of the two parameters $H$ and $r$, which are the distance between the donor-acceptor planes perpendicular to the membrane surface ($H$) and the projection of the distance vector on the plane of the acceptors, parallel to the membrane surface ($r$). $K_r$ provides a measure of the distribution of Py-SM in the AChR membrane (see Antollini et al. 1996). $K_r = 1$ implies a random distribution of probe molecules in the bilayer; in this case the probability of occupancy of sites by Py-SM at the lipid belt region is the same as the probability of Py-SM molecules being at any other location in the lipid bilayer, such that its weighting factor is simply the molar ratio of the two possible locations. $K_r < 1$ implies preferential location of Py-SM in the lipid belt region, and $K_r > 1$ indicates the exclusion of Py-SM from this region.

When FRET conditions were used after SMase treatment, the emission spectrum of the enzyme in buffer was recorded. The contribution of the intrinsic fluorescence of added SMase was found to be negligible ( < 1% of the total fluorescence), a fortunate condition which enabled the performance of experiments in the presence of SMase.

## Results

### Susceptibility of SM to SMase hydrolysis in native AChR membranes

In order to study the distribution of SM in AChR-rich membranes of *D. tschudii*, we treated these membranes with SMase, a soluble enzyme that hydrolyzes SM to phosphocholine and ceramide. As shown in Fig. 1, a plateau was reached after 5 min incubation, without further changes in the next 30–60 min. A maximal SM hydrolysis of ~60% was obtained under the present experimental conditions. The remaining 40% has been interpreted as SM located at the inner hemilayer of the membrane (Boegheim et al. 1983). Exponential fitting of the data yielded a $t_{1/2}$ of 0.82 min for SMase hydrolysis, which proceeded with an apparent rate of 20.7 nmol · min$^{-1}$.

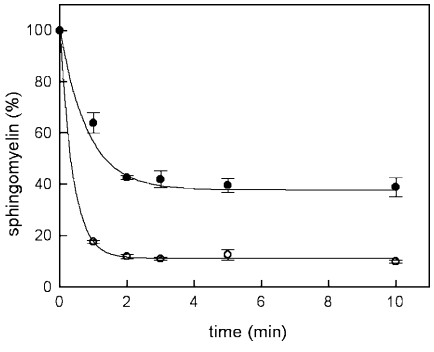


**Fig. 1.** Sphingomyelinase hydrolysis of native (*filled circles*) and 0.06% saponin-permeabilized (*open circles*) AChR-rich membranes from *D. tschudii*. Membranes were incubated with 0.5 U *B. cereus* SMase/mg protein at 37 °C in 20 mM HEPES buffer (pH 7.4) containing 150 mM NaCl and 0.25 mM $MgCl_2$. The reaction was stopped by addition of EDTA. Lipids were extracted in chloroform/methanol (1:2, v/v), separated by thin-layer chromatography, and quantified by phosphorus analysis. Results are mean values ± SD from four independent experiments

When SMase treatment was carried out in the presence of 0.06% saponin, SM hydrolysis was more exhaustive and proceeded faster than with the intact membrane (Fig. 1). After 1 min incubation, only 18% of the total SM remained in the membrane, and the reaction was almost complete within 2 min. The calculated $t_{1/2}$ of SMase action was 0.39 min; the rate of hydrolysis in this case was 43.6 nmol min$^{-1}$.

### The fatty acyl composition of SM is different in the two leaflets of the native AChR-rich membrane

Although PC and SM are esterically similar, at variance with PC, SM carries only one fatty acid chain per molecule, the second aliphatic chain corresponding to the long-chain base (sphingosine). Thus, the analytically determined fatty acid composition directly reflects the molecular species composition of this sphingolipid. Table 1 shows the molecular species composition of sphingomyelins in the inner (represented by SM) and outer (represented by ceramide) monolayers obtained upon treatment of native AChR membranes with SMase and chromatographic separation of SM and ceramide.

Statistically significant differences were observed between the fatty acid molecular species in SM in the inner and outer hemilayers of the membrane. Nervonic acid ($24{:}1^{\Delta 15c}$; 26%) followed by palmitic acid (16:0; 12%) were the principal components in the outer monolayer, where 60–80% of the total SM is located. In the inner monolayer, 16:0 amounted to 22% of the total fatty acid content while 24:1 represented about 16% and stearic (18:0) and oleic (18:1) acids each represented about 12% of the total. In the outer monolayer, long-chain ($C_{20}$–$C_{24}$), monoenoic fatty acids accounted for about 60% of the total, whereas the same percentage was found in the inner membrane leaflet for fatty acids with less than 20 C atoms. The ratio between saturated and unsaturated fatty acids was similar in the two leaflets of the membrane (Table 1).

### Topographical vicinity of protein and Py-SM in AChR-rich membranes

In addition to the asymmetric lipid distribution between inner and outer leaflets, the AChR membrane presents an additional asymmetry: that existing between annular lipids in the immediate microenvironment of the protein and the remaining bulk lipids (Marsh and Barrantes 1978; Barrantes 1993). Biochemical methods cannot differentiate between these two lipid regions. In this work a fluorescent analog of SM (Py-SM) is employed

**Table 1.** Composition (mol%) of sphingomyelins in the outer and inner leaflets of AChR-rich membranes from *D. tschudii*

| Fatty acid | Outer layer | Inner layer | Total membrane | |
|---|---|---|---|---|
| | Measured | Measured | Measured | Calculated[a] |
| 12:0 | 0.7 ± 0.1 | 0.7 ± 0.05 | 1.0 ± 0.5 | 0.7 ± 0.1 |
| 14:0 | 2.7 ± 0.2 | 1.7 ± 0.3 | 2.8 ± 0.8 | 2.3 ± 0.3 |
| 15:0 | 0.5 ± 0.04 | 0.8 ± 0.1 | 0.7 ± 0. 3 | 0.6 ± 0.1 |
| 16:0 | 11.6 ± 1.3 | 22.4 ± 2.1 | 13.7 ± 0.9 | 15.9 ± 1.2 |
| 16:1 | 3.5 ± 0.3 | 4.6 ± 0.5 | 3.6 ± 0.6 | 3.9 ± 0.5 |
| 17:0 | 0.9 ± 0.1 | 0.2 ± 0.01 | 0.8 ± 0.2 | 0.6 ± 0.05 |
| 18:0 | 8.0 ± 1.1 | 11.5 ± 0.9 | 7.5 ± 1.5 | 9.4 ± 1.1 |
| 18:1 | 8.3 ± 0.1 | 11.7 ± 1.1 | 7.2 ± 1.1 | 9.7 ± 0.7 |
| 19:0 | 2.7 ± 0.1 | 3.2 ± 0.03 | 1.7 ± 0.9 | 2.9 ± 0.1 |
| 20:0 | 5.5 ± 0.7 | 2.3 ± 0.2 | 3.7 ± 0.8 | 4.2 ± 0.5 |
| 20:1 | 2.0 ± 0.01 | 4.3 ± 0.6 | 1.7 ± 0.9 | 2.9 ± 0.3 |
| 21:0 | 0.9 ± 0.2 | 0.6 ± 0.05 | 0.7 ± 0.01 | 0.8 ± 0.05 |
| 22:0 | 5.4 ± 0.1 | 4.0 ± 0.9 | 4.3 ± 0.1 | 4.8 ± 0.3 |
| 22:1 | 8.7 ± 0.9 | 5.4 ± 0.4 | 10.8 ± 1.8 | 7.4 ± 0.7 |
| 23:0 | 4.0 ± 0.7 | 3.2 ± 0.8 | 3.5 ± 0.8 | 3.7 ± 0.9 |
| 23:1 | 2.6 ± 0.2 | 1.4 ± 0.6 | 3.3 ± 0.6 | 2.1 ± 0.4 |
| 24:0 | 5.5 ± 0.8 | 5.9 ± 0.9 | 8.0 ± 0.8 | 5.7 ± 0.7 |
| 24:1 | 26.3 ± 2.1 | 15.9 ± 1.8 | 24.9 ± 1.7 | 22.2 ± 1.9 |
| Total saturated fatty acids | 48.4 ± 0.9 | 56.5 ± 0.5 | 48.4 ± 1.8 | 51.6 ± 1.7 |
| Ratio sat/unsat | 0.9 ± 0.2 | 1.3 ± 0.2 | 0.9 ± 0.1 | 1.0 ± 0.05 |
| Total fatty acids with 20 carbon atoms or more | 60.9 ± 1.4 | 43.0 ± 1.1 | 60.9 ± 1.8 | 53.8 ± 2.3 |

[a]Calculated as the sum of the relative amounts of each fatty acid in the SM fractions in the outer and inner monolayers, respectively. Data are expressed as mean ± SD from three separate experiments ($n = 3$)

to investigate this point. First we explored the possibility of photoselecting the Py-SM molecules located in the annular region using resonance energy transfer (FRET) conditions from the protein emission. Figure 2A shows the good overlap between the protein emission and the Py-SM absorption spectra, indicating an efficient energy transfer between the donor Trp residues of the AChR protein and the pyrene-labeled acceptor lipid. The intrinsic fluorescence emission peak at 330 nm is characteristic of Trp emission maximum in nonpolar environments. Once Py-SM is incorporated into the AChR-rich membrane, at low concentrations the probe is predominantly monomeric, with emission maxima at 374 nm and 397 nm upon direct excitation at 346 nm (Fig. 2B). Only at higher (> 1.2 μM) concentrations does a broad excimer emission centered at ~475 nm become apparent (see below).

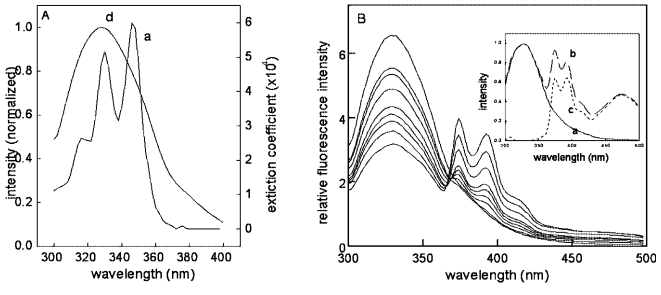


**Fig. 2.** **A** Spectral overlap between the emission spectrum of the *Torpedo* AChR membrane intrinsic protein fluorescence (*d*, donor) excited at 290 nm and the absorption spectrum of Py-SM (*a*, acceptor) shown as the molar extinction coefficient in the units indicated. Spectra were obtained at 20 °C. A value of $J = 3.40 \times 10^{-14}$ cm$^3$ M$^{-1}$ was obtained (see Materials and methods section). **B** Emission spectra of Py-SM in AChR-rich membrane under FRET conditions (exc.: 290 nm) as a function of acceptor concentration (from *top to bottom* at the 330 nm band: 0.08, 0.16, 0.23, 0.31, 0.39, 0.47, 0.55, and 0.62 μM). The pyrenyl probe/lipid ratio varied between 0.24 and 1.88%. *Inset*: normalized emission spectra of AChR membrane alone (*a*) and in the presence of Py-SM (*b*), in both cases excited at 290 nm, and difference spectrum (*c*), the result of subtracting (*b*) from (*a*). The protein concentration in the AChR membrane was 0.3 μM. Temperature was held at 20 °C

A fraction of the probe lies within energy transfer distance from the intrinsic fluorophores of the membrane protein, since upon excitation at 290 nm the emission of the former at 330 nm decreases while the pyrenyl probe emission increases as a function of acceptor concentration (Fig. 2B). This nonradiative process involves transfer of excitation energy that depends on the distance and orientation between donor and acceptor molecules (Förster 1948). From the donor intrinsic protein fluorescence and the absorption spectrum of the acceptor in Fig. 2A an overlap integral, $J$, of $3.40 \times 10^{-14}$ cm$^3$ M$^{-1}$ was experimentally determined. The calculated critical Förster distance, $R_0$, was 21 ± 2 Å. This is in agreement with literature values of about 20 Å for the tryptophan-pyrenylmaleimide pair (Narayanaswami et al. 1993).

## Thermal sensitivity of the pyrenyl excimer-monomer ($F_E/F_M$) ratio

Two nearest-neighbor pyrenyl probes, one in the excited state, can form an excimer provided they have the appropriate relative orientation and distance (Förster 1948). The rate of intermolecular excimer formation

depends on the concentration and mobility of the intervening molecules. The ability of pyrene and its derivatives to form excimers is a sensitive tool to assess dynamic properties in biological and artificial membranes (Sassaroli et al. 1990; Pap et al. 1995; Engelke et al. 1994, 1996). The excimer/monomer ratio can be used to characterize membrane structural domains and their dependence on temperature, lipid composition, and other external factors. We thus examined the temperature dependence of Py-SM fluorescence in the AChR membrane. Figure 3 shows typical donor-acceptor spectra in *T. marmorata* membranes in the temperature range between 5 and 45 °C.

As shown in Fig. 3 (inset), Py-SM in liposomes prepared from the endogenous lipids from AChR-rich membranes exhibited a higher $F_E/F_M$ ratio than that observed in the AChR membrane. This implies that the ability of Py-SM to undergo excimer formation is higher in liposomes than in the native, protein-containing AChR membrane, and by inference that the diffusion of the pyrene derivative in the membrane – its lateral mobility – is hindered in the presence of protein. This inference was confirmed by measuring excimer emission in the AChR membrane using FRET conditions. For Py-SM within energy transfer distance from the donor protein fluorophores the $F_E/F_M$ was even lower (~0.12) than that found in liposomes from endogenous lipid and in the bulk lipid of the AChR membrane. Thus the ability of Py-SM to undergo excimer formation in the 5–45 °C range is about 1.5- to 2-fold higher in the bulk lipid than in the lipid region close to the protein, where steric restrictions due to contact with the predominant AChR protein and/or reduced lateral diffusion appear to hinder successful excimer formation.

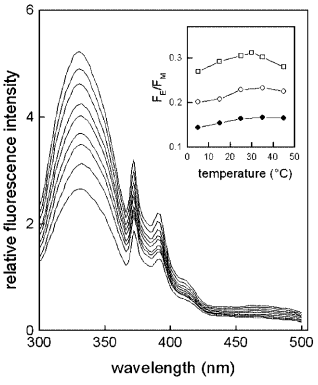


**Fig. 3.** Temperature dependence of Py-SM emission in AChR-rich membrane of *T. marmorata* under FRET conditions (excitation wavelength 290 nm). The concentration of Py-SM was fixed at 0.33 μM. Temperature was varied between 5 and 45 °C, with 5 °C increments. *Inset*: excimer/monomer ($F_E/F_M$) ratio of Py-SM emission as a function of temperature, using direct excitation of the probe (*open circles*, 346 nm) or FRET conditions (*filled circles*, 290 nm) in *T. marmorata* AChR membrane, and in liposomes prepared from AChR membrane lipids (*open squares*) excited at 346 nm. Protein concentration was 50 μg $mL^{-1}$. Py-SM was incorporated from an ethanol stock solution, incubated for 1 h, and washed by centrifuge in order to eliminate excess Py-SM

## Differences between excimer/monomer formation in bulk and AChR annular lipid regions

The ratio between excited-state pyrene dimer (excimer) and monomer pyrenyl fluorescence ($F_E/F_M$) reflects the intermolecular collisional frequency of the fluorophores, and the fluorophore concentration affects this parameter. We thus studied the concentration-dependent excimer formation both by direct excitation of the probe and under FRET conditions. As can be observed in Fig. 4, at very low Py-SM concentrations the $F_E/F_M$ ratio for Py-SM in the AChR membrane was higher upon direct excitation (~0.2) than that obtained under FRET conditions (~0.1), indicative of a higher fluidity in the bulk lipid than in the AChR microenvironment (Antollini et al. 1996) (Fig. 4). Furthermore, the gradient of the increment in the $F_E/F_M$ ratio at higher Py-SM concentrations is twice as high under FRET conditions as it is for direct excitation of the probe, suggesting that the Py-SM analog is preferentially partitioned in the protein-vicinal region.

## Relative affinity of Py-SM for the AChR lipid belt region

We extracted quantitative information on the relative topography of the intrinsic fluorescence-Py-SM donor-acceptor pair following the theoretical approach developed by Gutiérrez-Merino (Gutiérrez-Merino 1981a, 1981b; Gutiérrez-Merino et al. 1987, 1995). The values of FRET efficiency, $E$, for different acceptor surface densities were calculated as a function of $r$, $H$, and $K_r$ by parametric fitting of the theoretical predictions of FRET to the experimental data, weighting the probability of occurrence of donor-acceptor pairs at the lipid belt region relative to that of a random distribution. A value of $R_0$ of $21 \pm 2$ Å was obtained, calculated as indicated under Materials and methods. As shown in Fig. 5, the

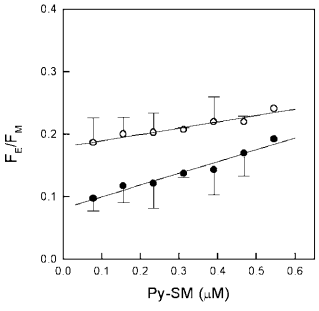


**Fig. 4.** Excimer/monomer ($F_E/F_M$) ratio as a function of Py-SM concentration in AChR membrane from *T. marmorata*, excited at 346 nm (direct excitation, *open circles*) and at 290 nm (FRET conditions, *filled circles*). The emission intensities of monomer ($F_M$) and excimer ($F_E$) were measured at 374 nm and 472 nm, respectively. Protein concentration was 50 μg $mL^{-1}$. The temperature was 20 °C. Results are mean values ± SD from four independent experiments

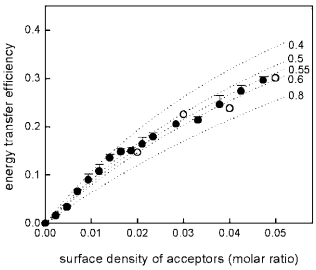


**Fig. 5.** Energy transfer efficiency between donor protein intrinsic fluorescence in the native *Torpedo* AChR membrane (*filled circles*) or in affinity purified and lipid reconstituted AChR (*open circles*) and Py-SM as a function of the acceptor density. A constant concentration of the fluorescent donor was titrated with increasing concentrations of the fluorescent acceptor. The curves correspond to the theoretical fits to different $K_r$ values calculated according to Gutiérrez-Merino (1981a, 1981b) for $H = 10$ Å, $r = 10$ Å, and $R_0 = 21$ Å. Results are mean values ± SD from four independent experiments. Protein concentration was 50 μg mL$^{-1}$; Py-SM concentration varied between 0.08 and 1.68 μM. Temperature was kept at 20 °C

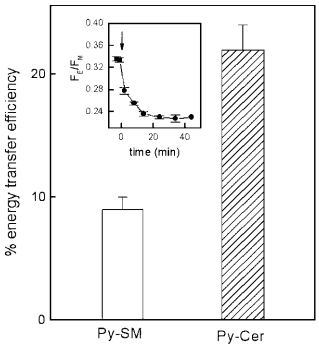


**Fig. 6.** FRET efficiency between intrinsic fluorophores of AChR membrane and Py-SM or its hydrolysis product, Py-Cer, upon SMase treatment of the membrane. The protein concentration was 50 μg mL$^{-1}$ and Py-SM concentration was 0.33 μM. Temperature was 20 °C. Results are mean values ± SD from three independent experiments. *Inset*: time course of SMase action on Py-SM-labeled AChR-rich membranes (*filled circles*), as followed by changes in pyrenyl excimer/monomer ratio. The *arrow* shows the addition of SMase. Temperature was kept at 37 °C

data are well described by the theoretical predictions of FRET with a single plane of acceptors, and from the best fit of the experimental data to values of $r = 10$ Å and $H = 10$ Å, yielding a value of $d = 14$ Å. As expected for a constant molar ratio of the donor AChR protein in the membrane, $E$ varied as a function of Py-lipid acceptor surface density (Fig. 5). A value of $K_r \approx 0.55$ relative to the average lipid population in the membrane was obtained for Py-SM, thus indicating a moderate affinity of this lipid for the membrane-bound AChR.

The present study was carried out on native AChR membrane, which although rich in AChR protein does leave open the possibility that the results reflect SM interaction with a membrane protein other than the AChR. In order to discard this possibility, we conducted the same series of experiments with affinity purified AChR reconstituted into liposomes made from *Torpedo* lipid extracts. Figure 5 shows this series of experiments. No difference in the efficiency of FRET between Trp(s) and Py-SM as a function of probe concentration was observed between the two preparations. A fit to both experimental data sets could be obtained with the same $K_r$ (~0.55), suggesting that the data obtained with native AChR faithfully reflects the interaction of SM with the AChR membrane microenvironment, which exhibits a moderate affinity for SM.

### Fluorescence changes upon SMase treatment of AChR-rich membranes

SMase treatment has been shown to deplete SM from the outer leaflet of the membrane (Jansson et al. 1993). Upon SMase treatment, Py-SM is converted to phosphorylcholine and Py-ceramide, an *N*-acyl derivative of SM. We treated *T. marmorata* membranes with SMase and calculated the FRET efficiency before and after enzymatic hydrolysis (Fig. 6). The hydrolytic cleavage occurred within minutes, and resulted in a marked increase in the efficiency of FRET between protein and the resulting pyrenyl-ceramide, suggesting both a higher affinity of Py-Cer for the donor protein and/or a greater accessibility of this lipid to the lipid microenvironment of the AChR (Fig. 6).

A progressive decrease of the $F_E/F_M$ ratio was observed upon SMase treatment (Fig. 6, inset). This reinforces the view that the resulting Py-ceramide species exhibits higher affinity/greater accessibility for the protein than the parental Py-SM compound.

## Discussion

### Asymmetric lipid distribution in the AChR-rich membrane

The aminophospholipids PE and PS, together with phosphatidylinositol, are localized mainly in the inner leaflet of the plasmalemma, whereas PC and SM are found predominantly in the outer leaflet in most mammalian cells (Op den Kamp 1979; Devaux 1991). In mouse synaptic plasma membranes, the outer monolayer is more fluid than the inner leaflet (Schroeder et al. 1988; Wood et al. 1989), an observation that is correlated with the marked predominance (88%) of cholesterol in the inner, cytoplasmic hemilayer (Wood et al. 1990). Scher and Bloch (1993) determined that AChR-rich membranes where receptor clusters occur in rat myotubes exhibit phospholipid asymmetry; at least 77% of the plasma membrane aminophospholipids PS and PE associated with the AChR clusters was located in the inner, cytoplasmic leaflet of the membrane. Using chemical derivatization with trinitrobenzenesulfonate (TNBS) and hydrolysis by phospholipase C, we have previously reported sidedness in the distribution of the major phospholipids in AChR-rich membranes of the

fish electric organ from *D. tschudii* and *T. marmorata* (Bonini de Romanelli et al. 1990). However, both treatments fall short of providing comprehensive information on the topography of phospholipids within the bilayer, and in particular of SM, because a nonspecific phospholipase was used and trinitrobenzenesulfonate reacts with aminophospholipids only. In another study from our laboratory, we found that fluorescent derivatives of PC and PE are preferentially located in the outer, exofacial leaflet of the membrane (Gutiérrez-Merino et al. 1995).

Here we concentrate on SM, firstly using an SM-specific phospholipase to study its overall topography in the membrane, an approach that is well documented (Roelofsen 1982). SMase treatment has been shown to deplete SM (and cholesterol) in the outer leaflet of the membrane (Jansson et al. 1993). By comparing the SM-specific hydrolase products from native membranes and saponin-permeabilized membranes, SM was found to be asymmetrically distributed between the two leaflets of the bilayer in the AChR-rich membrane. About 18% of SM was not cleaved even after 1 h reaction; a plateau was reached after only 2 min (Fig. 1). If ~18% of non-hydrolyzable SM is in the *outer* leaflet, this implies that, altogether, $60 + 18 = 78\%$ of SM is located in the outer hemilayer. Should 18% of the non-hydrolyzable SM be in the *inner* hemilayer, still 60% of the total SM would be located in the exofacial leaflet of the membrane. The basic conclusion remains the same: SM is asymmetrically distributed between the two hemilayers, the outer one having a higher percentage (60–78%) of SM. In erythrocytes, the presence of SM in the outer leaflet has been suggested to increase the rigidity of the membrane (Deuticke 1977). Although quantitatively a minor component of the AChR membrane, SM may play a structural role related, at least in part, to the mismatch between the choline-containing sphingosine base of SM and the acyl chain, making itself apparent in the protrusion of the SM head group above the plane of the polar head region of the rest of the lipid bilayer (Levin et al. 1985).

## Asymmetric distribution of fatty acyl molecular species in SM of AChR-rich membranes

We next focused on the molecular species of SM in the AChR-rich membrane. First we found that this lipid is unique in terms of its fatty acid composition, lacking the most usual species present in other phospholipids from AChR-rich membranes (Rotstein et al. 1987) and having relatively unusual species instead (cf. Table 1). We then analyzed the transbilayer distribution of molecular species of SM in each membrane leaflet, and found that they are also asymmetrically distributed (Table 1). There are few reports on transbilayer asymmetry of fatty acid molecular species in biological membranes, and only in a few instances has this been measured for SM. In one such case, asymmetry was found for SM molecular species in the erythrocyte (Boegheim et al. 1983). In *T. marmorata* AChR-rich membranes, the relative proportion of saturated and unsaturated fatty acids is about equal in the two leaflets of the bilayer, though the absolute amount of short-chain, saturated fatty acids is slightly higher in the inner leaflet (cf. Table 1). This contrasts with mammalian blood cells, for instance, where the inner leaflet contains higher proportions of polyunsaturated fatty acids than the outer leaflet (Lagarde et al. 1982; Naughton et al. 1988).

## Physical contact between protein and a fraction of Py-SM in the AChR membrane

FRET is the nonradiative process by which energy is transferred from an emitting fluorophore (the donor) to a suitable acceptor by long-range dipole-dipole coupling (Förster 1948). We have exploited this fluorescence modality to measure the topographical relationship between the protein and the protein-adjacent fluorescent SM analogue. The good spectral overlap between the Trp emission and the pyrenyl absorption spectrum has permitted the use of FRET techniques to learn about the location of fluorophores in membrane proteins (e.g. Bastiaens et al. 1990). Our experimental findings show that a subpopulation of the Py-SM probe lies within FRET distance from the intrinsic fluorophores of the AChR-rich membrane protein, since upon excitation at 290 nm the emission of the former at ~330 nm decreases while the pyrenyl probe emission increases as a function of acceptor concentration (Fig. 2). The acceptor Py-SM molecules lie within a calculated radius of ~14 Å from the AChR Trp residues (i.e. establishing successful FRET), and a calculated vertical distance of about 10 Å separates donor and acceptor planes in the direction normal to the membrane surface.

Pyrene and its derivatives are known to undergo an excited state reaction in which two molecules, one in the excited state and the other in the ground state, interact to form an excited-state dimer (excimer) with a fluorescence emission red-shifted with respect to the monomer (Förster 1948). The monomer to excimer fluorescence intensity ratio can be related to the kinetic constants for the formation and deactivation of these states by the relationship:

$$F_E/F_M = (k_E/k_M)k_a\tau_0 \quad (2)$$

where $F_E$ and $F_M$ are the fluorescence intensities of the excimer and monomer, respectively, $k_E/k_M$ the corresponding ratio of the rate constants for excimer and monomer fluorescence, $k_a$ the rate constant for excimer formation, and $\tau_0$ the excimer fluorescence lifetime in the absence of dissociation. The radiative constants and $\tau_0$ have been found to be essentially independent of temperature, whereas $F_E/F_M$ changes in a temperature-sensitive manner with the fluidity of the viscous medium (Zachariasse et al. 1980). The mechanism of

pyrenyl-compound excimer formation in the low monomer concentration range is dynamic in the case of PC liposomes (Barenholz et al. 1996).

When we examined the temperature dependence of $F_E/F_M$, we found no indication of phase transition in the AChR-rich membrane in the temperature range studied (Fig. 3). Electric fish live at rather low temperatures, and probably in situ membrane lipids are in a liquid-crystalline phase in the temperature range studied here. Cholesterol, which is known to have a condensing effect above phase transition temperatures, is relatively abundant in the AChR-rich membrane, reaching phospholipid/cholesterol molar ratios ≥1.3 (Rotstein et al. 1987). This corresponds to a total of about 230 phospholipids and 130 cholesterol molecules per AChR molecule in a typical membrane preparation (Barrantes 1989). The lack of a sharp thermotropic transition in the AChR membrane can also be attributed to the heterogeneous lipid composition of these membranes (Rotstein et al. 1987).

The absolute $F_E/F_M$ values for Py-SM in the AChR membrane excited at 346 nm, reporting on excimer formation in the bulk lipid, were ~2-fold higher than those obtained by measuring excimer emission in the AChR membrane using FRET conditions with 290 nm excitation, which should report on the protein-associated lipid region (Fig. 3). Thus the ability of Py-SM to successfully undergo excimer formation is about 2-fold lower in the lipid region close to the protein, where contact with the AChR surface appears to hinder such formation. Lateral and rotational diffusion rates of the pyrenyl derivative may become lower than the fluorescence decay rate of its excited state (~0.02 $ns^{-1}$), thus reducing the probability of excimer formation. Barenholz et al. (1996) have reported that the steric factor is most important in reducing the ability of pyrene derivatives to interact in a productive manner to form excimers. In the present case the most likely explanation is that the AChR protein imposes a marked hindrance to excimer formation, in agreement with the notion that the protein restricts the mobility of those lipids close to its surface (Engelke et al. 1994, 1996). This is in full agreement with our earlier ESR and fluorescence spectroscopy studies in which we demonstrated (1) protein-induced reduction of rotational correlation time of spin-labeled fatty acids (Marsh and Barrantes 1978) and phospholipids (Marsh et al. 1981) in AChR-rich membranes, and (2) the proximity of lipid and AChR protein by intrinsic fluorescence quenching studies (Barrantes 1978; Marsh and Barrantes 1978). The present results are in agreement with other studies in which the physical state of the AChR lipid belt region was investigated with Laurdan, a probe that does not exhibit any preferential affinity for the AChR protein (Antollini et al. 1996; Antollini and Barrantes 1998). We found that only one *ordered* (from the point of view of molecular axis rotation)-*liquid* (from the point of view of lateral diffusion) lipid phase is present in the native AChR membrane, and that AChR annular lipid differs structurally and dynamically from the bulk bilayer lipid in terms of polarity and molecular motion.

Remarkably, the gradient of the $F_E/F_M$ slope as a function of Py-SM concentration was 2-fold higher under FRET conditions than under conditions using direct excitation of the probe. This can be explained by the fact that Py-SM shows a relative affinity for the AChR lipid microenvironment. Taking into account the transmembrane radii of AChR protein and lipid (~29 Å and 4.8 Å, respectively), the number of lipids in the first lipid shell around the AChR is ~44 (Ellena et al. 1983). If one further considers the lipid composition of the *T. marmorata* AChR membrane (Bonini de Romanelli et al. 1987), and assuming no selectivity of any lipid class for the AChR, it follows that an average of 2.2 SM molecules would be located in the first shell of lipids surrounding the protein. With only two molecules, it is clear why it is so difficult for them to collide and form excimers in this region. A higher affinity of SM for the AChR microenvironment would imply a higher average number of SM molecules in this region and consequently a higher probability of excimer formation.

The actual affinity of Py-SM for the AChR annular region was calculated from a different set of experiments. When $E$ was analyzed in terms of a simple model considering only one shell of annular lipid and a bulk lipid region (Antollini et al. 1996) for a set of different $K_r$ values (the relative affinity constant of Py-SM for the protein donor), an average $K_r$ value of 0.55 could be calculated, indicating that Py-SM indeed exhibits a moderate selectivity for the AChR first-shell lipid region in comparison to the bulk lipid in the native AChR membrane. Sassaroli et al. (1990) emphasized that pyrenyl derivatives, unlike more polar fluorophores, mimic more closely the natural, unlabeled precursor lipid.

The increase in the efficiency of energy transfer between Trp and Py-Cer as compared to that between Trp and Py-SM may be related to a higher affinity of the former lipid analog for the AChR. In addition, a greater accessibility of the ceramide derivative to sites at the lipid-protein interface can be invoked. To date, two different types of sites for lipids are postulated at the AChR-lipid interface, non-annular sites for cholesterol and free fatty acids, and annular sites for both phospholipids and fatty acids (Jones and McNamee 1988; Antollini and Barrantes 1998). Furthermore, ceramide is a single-chain, neutral lipid, structurally similar to a free fatty acid (Kamp and Hamilton 1993). In reconstituted systems, Ellena et al. (1983) found that fatty acids have ~4-fold higher affinity for the membrane-bound *Torpedo* AChR as compared to PC. We also determined the relative affinity of lipid analogs for the whole *T. californica* AChR and purified transmembrane AChR peptides (Barrantes et al. 2000). We found that a stearic acid analogue displayed affinities of 9:1 and 0.7:1 relative to a cholestane and an androstane analogue, respectively. In a more recent study from our laboratory, we found that different fatty acids share a common site on the AChR protein (Antollini and Barrantes 2002).

Taken together, the data suggest that ceramide exhibits a higher affinity for the AChR receptor protein, and may bind to sites at the lipid-protein interface different from those for SM, perhaps the same as those for fatty acids. Further experiments are underway in our laboratory to test this hypothesis.

**Acknowledgements** Thanks are due to Prof. Dr.M. Prieto for critical reading of the manuscript. This work was supported in part by grants from the Universidad Nacional del Sur, the Agencia Nacional de Promoción Científica (FONCYT), Ministerio de Salud, Argentina, and FIRCA 1-RO3-Tw 01225-01 to F.J.B.

## References

Antollini SS, Barrantes FJ (1998) Disclosure of discrete sites for phospholipid and sterols at the protein-lipid interface in native acetylcholine receptor-rich membrane. Biochemistry 37:16653–16662

Antollini SS, Barrantes FJ (2002) Unique effects of different fatty acid species on the physical properties of the *Torpedo* acetylcholine receptor membrane. J Biol Chem 277:1249–1254

Antollini SS, Soto MA, Bonini de Romanelli I, Gutiérrez-Merino C, Sotomayor P, Barrantes FJ (1996) Physical state of bulk and protein-associated lipid in nicotinic acetylcholine receptor-rich membrane studied by Laurdan generalized polarization and fluorescence energy transfer. Biophys J 70:1275–1284

Arvidson GAE (1968) Structural and metabolic heterogeneity of rat liver glycerophosphatides. Eur J Biochem 4:478–486

Barenholz Y, Thompson TE (1980) Lateral organization of pyrene-labeled lipids in bilayers as determined from the derivation from equilibrium between pyrene monomers and excimers. Biochim Biophys Acta 604:129–158

Barenholz Y, Cohen T, Haas E, Ottolenghi M (1996) Lateral organization of pyrene-labeled lipids in bilayers as determined from the derivation from equilibrium between pyrene monomers and excimers. J Biol Chem 271:3085–3090

Barrantes FJ (1978) Agonist-mediated changes of the acetylcholine receptor in its membrane environment. J Mol Biol 124:1–26

Barrantes FJ (1982) Interactions of the membrane-bound acetylcholine receptor with the non-receptor peripheral *v*-peptide. In: Hucho F (ed) Neuroreceptors. de Gruyter, Berlin, pp 315–328

Barrantes FJ (1989) The lipid environment of the nicotinic acetylcholine receptor in native and reconstituted membranes. Crit Rev Biochem Mol Biol 24:437–478

Barrantes FJ (1993) The lipid annulus of the nicotinic acetylcholine receptor as a locus of structural-functional interaction. In: Watts A (ed) New comprehensive biochemistry, vol. 26. Elsevier, Amsterdam, pp 231–257

Barrantes FJ, Sakmann B, Bonner R, Eibl H, Jovin TM (1975) 1-Pyrene-butyrylcholine: a fluorescence probe for the cholinergic system. Proc Natl Acad Sci USA 72:3097–4001

Barrantes FJ, Antollini SS, Blanton MP, Prieto M (2000) Topography of nicotinic acetylcholine receptor membrane-embedded domains. J Biol Chem 275:37333–37339

Bastiaens P, de Beus A, Lacker M, Somerharju P, Vaukhonen M, Eisinger J (1990) Resonance energy transfer from a cylindral distribution of donors to a plane of acceptors. Location of apo-B100 protein on the human low-density lipoprotein particle. Biophys J 58:665–675

Bligh EB, Dyer WJ (1959) A rapid method of total lipid extraction and purification. Can J Biochem Physiol 37:911–917

Boegheim JPJ Jr, Van Linde M, Op den Kamp JAF, Roelofsen B (1983) The sphingomyelin pools in the outer and inner layer of the human erythrocyte membrane are composed of different molecular species. Biochim Biophys Acta 735:438–442

Bonini de Romanelli IC, Roccamo de Fernández AM, Barrantes FJ (1987) Extraction of peripheral proteins is accompanied by selective depletion of certain glycerophospholipid classes and changes in the phosphorylation pattern of acetylcholine receptor-rich membrane proteins. Biochem J 245:111–118

Bonini de Romanelli IC, Aveldaño MI, Barrantes FJ (1990) Asymmetric distribution of phopholipids in acetylcholine receptor-rich membranes from *T. marmorata* electric organ. Int J Biochem 22:785–789

Brown RE (1998) Sphingolipid organization in biomembranes: what physical studies of model membranes reveal. J Cell Sci 111:1–9

Deuticke B (1977) Properties and structural basis of simple diffusion pathways in the erythrocyte membrane. Rev Physiol Biochem Pharmacol 78:1–97

Devaux PF (1991) Static and dynamic lipid asymmetry in cell membranes. Biochemistry 30:1163–1173

Devaux PF (1992*)* Protein involvement in transmembrane lipid asymmetry. Annu Rev Biophys Biomol Struct 21:417–439

Ellena JF, Blazing MA, McNamee MG (1983) Lipid-protein interactions in reconstituted membranes containing acetylcholine receptor. Biochemistry 22:5523–5535

Engelke M, Behmann T, Ojeda F, Diehl HA (1994) Heterogeneity of microsomal membrane fluidity: evaluation using intrinsic tryptophan energy transfer to pyrene probes. Chem Phys Lipids 72:35–40

Engelke M, Bojarski P, Diehl HA, Kubicki A (1996) Protein-dependent reduction of the pyrene excimer formation in membranes. J Membr Biol 153:117–123

Folch J, Lees MB, Sloane-Stanley GH (1957) A simple method for the isolation and purification of total lipids from animal tissues. J Biol Chem 226:497–509

Förster Th (1948) Intermolecular energy migration and fluorescence. Ann Phys 2:55–75

González-Ros JM, Llanillo M, Paraschos A, Martinez-Carrion M (1982) Lipid environment of acetylcholine receptor from *Torpedo californica*. Biochemistry 21:3467–3474.

Gutiérrez-Merino C (1981a) Quantitation of the Föster energy transfer for two-dimensional systems. I. Lateral phase separation in unilamellar vesicles formed by binary phospholipids mixtures. Biophys Chem 14:247–257

Gutiérrez-Merino C (1981b) Quantitation of the Föster energy transfer for two-dimensional systems. II. Protein distribution and aggregation state in biological membranes. Biophys Chem 14:259–266

Gutiérrez-Merino C, Munkonge F, Mata AM, East JM, Levinson BL, Napier RM, Lee AG (1987) The position of the ATP binding site on the $(Ca^{2+} + Mg^{2+})$-ATPase. Biochim Biophys Acta 897:207–216

Gutiérrez-Merino C, Molina A, Escudero B, Diez A, Laynez J L (1989) Interaction of local anesthetics dibucaine and tetracaine with sarcoplasmic reticulum membranes. Differential calorimetry and fluorescence studies. Biochemistry 28:3398–3406

Gutiérrez-Merino C, Bonini de Romanelli I, Pietrasanta L, Barrantes FJ (1995) Preferential distribution of the fluorescent phospholipid probes NBD-phosphatidylcholine and rhodamine-phosphatidyletanolamine in the exofacial leaflet of acetylcholine receptor rich membranes from *Torpedo marmorata*. Biochemistry 34:4846–4855

Hannun YA, Obeid LM (1995) Ceramide: an intracellular signal for apoptosis. Trends Biochem Sci 20:73–77

Hartig PR, Raftery MA (1979) Preparation of right side-out acetylcholine receptor enriched intact vesicles from *Torpedo californica* electroplaque membranes. Biochemistry 18:1142–1150

Homan R, Eisenberg M (1985) A fluorescence quenching technique for the measurement of paramagnetic ion concentrations at the membrane/water interface. Intrinsic and X537A-mediated cobalt fluxes across lipid bilayer membranes. Biochim Biophys Acta 812:485–492

Jacobson K, Dietrich C (1999) Looking at lipids rafts? Trends Cell Biol 9:87–91

Jansson C, Harmala A-S, Toivola DM, Slotte JP (1993) Effects of the phospholipids environment in the plasma membrane on

receptor interaction with the adenylyl cyclase complex of intact cells. Biochim Biophys Acta 1145:311–319
Jones OT, McNamee MG (1988) Annular and nonannular binding sites for cholesterol associated with the nicotinic acetylcholine receptor. Biochemistry 27:2364–2374
Kamp F, Hamilton JA (1993) Movement of fatty acids, fatty acids analogues and bile acids across phospholipid bilayers. Biochemistry 32:11074–11086
Koval M, Pagano RE (1991) Intracellular transport and metabolism of sphingomyelin. Biochim Biophys Acta 1082:113–125
Lacorazza HD, López RA, Venera GD, Biscoglio De Jimenez Bonino M (1996) Localization of histidine residues relevant for the binding of alpha-bungarotoxin to the acetylcholine receptor alpha-subunit in V8-proteolytic fragments. Neurochem Int 28: 557–567
Lagarde M, Guichardant M, Menashi S, Crawford N (1982) The phospholipid and fatty acid composition of human platelet surface and intracellular membranes isolated by high voltage free flow electrophoresis. J Biol Chem 257:3100–3104
Lakowicz JR (1999) Principles of fluorescence spectroscopy. Plenum, New York
Levin IW, Thompson TE, Barenholz Y, Huang C (1985) Two types of hydrocarbon chain interdigitation in sphingomyelin bilayers. Biochemistry 24:6282–6286
Lowry OH, Rosebrough NJ, Farr AL, Randall RJ (1951) Protein measurement with the Folin phenol reagent. J Biol Chem 193:265–275
Marquez J, Iriarte A, Martínez-Carrión M (1989) Covalent modification of a critical sulfhydryl group in the acetylcholine receptor: cysteine-222 of the alpha-subunit. Biochemistry 28:7433–7439
Marsh D, Barrantes FJ (1978) Immobilized lipid in acetylcholine receptor-rich membranes from *Torpedo marmorata*. Proc Natl Acad Sci USA 75:4329–4333
Marsh D, Watts A, Barrantes FJ (1981) Phospholipid chain immobilization and steroid rotational immobilization in acetylcholine receptor-rich membranes from *Torpedo marmorata*. Biochim Biophys Acta 645:97–101
Morrison WR, Smith LM (1964) Preparation of fatty acid methylesters and dimethylacetals from lipids with boron fluorides methanol. J Lipid Res 5:600–608
Narayanaswami V, Kim J, McNamee MG (1993) Protein-lipid interactions and *Torpedo californica* nicotinic acetylcholine receptor function. 1. Spatial disposition of cysteine residues in the $\gamma$ subunit analyzed by fluorescence-quenching and energy-transfer measurement. Biochemistry 32:12413–12419
Naughton JM, Sinclair AJ, O'Dea K, Steel MS (1988) Effects of dietary butter enrichment on the fatty acid distribution of phospholipid fractions isolated from rat platelets and aortae. Biochim Biophys Acta 962:166–172
Op den Kamp JAF (1979) Lipid asymmetry in membranes. Annu Rev Biochem 48:47–71
Pap EHW, Hanicak A, van Hoek A, Wirtz KWA, Visser AJWG (1995) Quantitative analysis of lipid-lipid and lipid-protein interactions in membranes by use of pyrene-labeled phosphoinositides. Biochemistry 34:9118–9125
Roelofsen B (1982) Phospholipases as tools to study the localization of phospholipids in biological membranes. A critical review. J Toxicol Toxin Rev 1:87–197
Rotstein NP, Arias HR, Aveldaño MI, Barrantes FJ (1987) Composition of lipids in elasmobranch electric organ and acetylcholine receptor membranes. J Neurochem 49:1333–1340
Rouser G, Fleischer S, Yamamoto A (1970) Two-dimensional thin-layer chromatographic separation of polar lipids and determination of phospholipids by phosphorus analysis of spots. Lipids 5:494–497
Sassaroli M, Vauhkonen M, Perry D, Eisinger J (1990) Lateral diffusivity of lipid analogue excimeric probes in dimyristoylphosphatidylcholine bilayers. Biophys J 57:281–290
Scher MG, Bloch RJ (1993) Phospholipid asymmetry in acetylcholine receptor clusters. Exp Cell Res 208:485–491
Schroeder F, Morrison WJ, Gorka C, Wood WG (1988) Transbilayer effects of ethanol on fluidity of brain membrane leaflets. Biochim Biophys Acta 946:85–94
Venera GD, Testai FD, Peña C, Biscoglio de Jiménez Bonino MJ (1997) Involvement of histidine 134 in the binding of alpha-bungarotoxin to the nicotinic acetylcholine receptor. Neurochem Int 31:151–157
Vénien C, Le Grimellec C (1988) The involvement of cytoskeletal proteins in the maintenance of phospholipid topology in renal brush-border membranes. Biochim Biophys Acta 946:307–314
Wood WG, Gorka C, Schroeder F (1989) Acute and chronic effects of ethanol on transbilayer membrane domains. J Neurochem 52:1925–1930
Wood WG, Schroeder F, Hogy L, Rao AM, Nemecz G (1990) Asymmetric distribution of a fluorescent sterol in synaptic plasma membranes: effects of chronic ethanol consumption. Biochim Biophys Acta 1025:243–246
Zachariasse KA, Kühnle W, Weller A (1980) Intermolecular excimer fluorescence as a probe of fluidity changes and phase transitions in phosphatidylcholine bilayers. Chem Phys Lett 73:6–11